

# A DISTRIBUTED PARAMETERS MODEL FOR SOLAR CELLS

by

G. C. Jain and F. M. Stuber

Department of Electrical Engineering

Rice University, Houston, Texas

## Abstract

The distributive circuit element model consists of a chain of T elements. The elemental model is made up of series and shunt paths. The sheet resistance of the diffused layer constitutes the series path. The shunt paths are three fold, consisting of the diode together with a series resistance, a conductance and a light generated current source. For a given cell, the parameters used in the model can be obtained by measuring the potential profiles for reverse -biased, forward-biased and short-circuited illuminated conditions and feeding the data obtained from the measurements in the solution of the differential equations for the model. The model has been successfully employed to compute optimum gridding for the cell.

GPO PRICE \$ \_\_\_\_\_  
CFSTI PRICE(S) \$ \_\_\_\_\_  
Hard copy (HC) 1.00  
Microfiche (MF) 150

REF ID: A6

FACILITY FORM 602

N66 33403	(THRU)
22	1
CR-74027	03
(ACCESSION NUMBER)	(CODE)
(PAGES)	(CATEGORY)
(NASA CR OR TMX OR AD NUMBER)	

## INTRODUCTION

Resistive components in solar cells cause power dissipation. The loss due to the sheet resistance of the diffused layer can be minimized by a grid structure contact. The purpose of this work is the derivation of a model for a solar cell suitable for the accurate design of an optimal grid. Wolf<sup>1</sup> studied the grid structure of a solar cell using a lumped parameter model. The optimized grid configuration based on the model did not conform too well with the experimental results. Lamorte<sup>2</sup> assumed a grid configuration and showed with the help of a distributed parameter model that the grid configuration was satisfactory.

In this work a new distributed parameters model is derived for an ungridded cell. It consists of a distributed resistance in the series path and shunted diodes with series resistance and current sources per differential cell length in the shunt paths. The analysis of cells based on this model leads to a system of three coupled, non-linear, first order differential equations. A solution was reached by computer methods. Data for the solution of the equations was obtained from measurements of the potential profiles along the length of the cell under reverse-biased, forward-biased and illuminated short circuited conditions. An optimized grid structure for the cell has been obtained by maximizing the power density.

## SETTING UP OF THE MODEL

The model of the solar cell is set up under the following assumptions:

- I) The cells are rectangular in shape, with the diffused layer exposed to the radiation.
- II) The resistance of the base layer is negligibly small.
- III) The bottom of the base layer has a metallic contact over all the area.
- IV) A rectangular contact strip is provided at one end of the diffused layer.
- V) The length of the exposed area of the cell  $W$  is much larger than the width of the contact  $W_c$ .
- VI) The contact resistances of the metallic contacts are negligibly small.
- VII) The cells are homogeneous or there are no potential variations along the y-direction in Figure 1 for the cell under illuminated, short-circuited conditions.
- VIII) The cells are assumed to have a depth of one unit length along the y-direction.

When exposed to radiation, the solar cell along its length may be considered to be made up of an infinite number of basic units of the type shown in Figure 2a. The load resistance is connected across the unit at  $x = W$ .

In the basic unit, the diffused layer is represented by a distributed constant resistance  $\rho$  per unit length.  $g$  is the shunt conductance per unit length;  $r$  is the series resistance of the diode per unit length;  $J_R$  is the light generated or radiation current density and is proportional to the intensity of light if the spectral distribution of the radiation is not varied.  $J_R$  is the same for all units. The diodes in the various units are assumed to be identical and are characterized by their reverse saturation current density  $J_o$ , which is determined by the properties of the material.  $J_D$  is the current density through the diode.

The equations describing this model are

$$\frac{dV(x)}{dx} = -\rho I(x) \quad (1)$$

$$\frac{dI(x)}{dx} = -g V(x) - J_D(x) + J_R \quad (2)$$

$$V(x) = V_D(x) + J_D(x) r \quad (3)$$

According to the Schokley diode equation

$$J_D(x) = J_o (e^{a V_D(x)} - 1) \quad (4)$$

or

$$V_D(x) = \frac{1}{a} \ln \left( \frac{J_D(x)}{J_o} + 1 \right)$$

Hence equation 3 changes to

$$V(x) = \frac{1}{a} \ln \left( \frac{J_D(x)}{J_o} + 1 \right) + J_D(x) r \quad (5)$$

Differentiating

$$\frac{dV}{dx} = \frac{1}{a} \frac{1}{\frac{J_D(x)}{J_o} + 1} \frac{1}{J_o} \frac{dJ_D}{dx} + r \frac{dJ_D}{dx}$$

or

$$\frac{dV}{dx} = \left( \frac{1}{a(J_D + J_o)} + r \right) \frac{dJ_D}{dx} \quad (6)$$

Substituting Equation 6 in Equation 1

$$\frac{dJ_D(x)}{dx} = \frac{-\rho a [J_D(x) + J_o]}{1 + r a [J_D(x) + J_o]} I(x) \quad (7)$$

Rationalizing Equations 7, 1 and 2 by putting  $\frac{x}{W} = \xi$

$$\frac{d J_D(\xi)}{d \xi} = - \frac{\rho W [J_D(\xi) + J_0]}{1 + r a [J_D(\xi) + J_0]} I(\xi) \quad (8)$$

$$\frac{d I(\xi)}{d \xi} = - W [g V(\xi) + J_D(\xi) - J_R] \quad (9)$$

$$\frac{d V(\xi)}{d \xi} = - \rho I(\xi) W \quad (10)$$

Equations 8, 9 and 10 are a system of nonlinear, coupled first order differential equations. There are three boundary conditions necessary for a unique solution. In order to determine  $I(\xi)$ ,  $J_D(\xi)$  and  $V(\xi)$  from the above equations it is necessary to know the parameters  $\rho$ ,  $g$ ,  $r$ ,  $J_0$  and of course,  $J_R$  for a given illumination level.

#### Determination of $J_R$ .

The radiation current density is not directly accessible to measurements but can be estimated from the open circuit voltage of the cell. Under illuminated condition but no load or battery connected across the cell,  $I(\xi) = 0$ . Hence in each unit of the model,  $J_R$  flows through the shunt conductance  $g$  and the series connection of the resistance  $r$  and the diode causing an open circuit voltage  $V_{OC}$ . The current flowing through  $g$  is seen to be several orders of magnitude smaller than  $J_D$  and can be neglected. Hence  $J_R = J_D$  for open circuit. Therefore, making use of Eq. 4

$$J_R = J_0 \left[ e^{a(V_{OC} - r J_R)} - 1 \right]$$

or

$$\frac{1}{a} \ln \left( \frac{J_R}{J_0} + 1 \right) - (V_{OC} - r J_R) = 0 \quad (11)$$

For a measured value of  $V_{OC}$ ,  $J_R$  can be computed numerically from the transcendental Eq. 11, provided  $J_0$  and  $r$  are known.

#### Determination of $\rho$ and $g$ .

The parameters  $g$  and  $\rho$  can be investigated by considering the unilluminated cell under reverse-biased condition. The model for this case is given in Figure 2b. The cell along its length is equivalent to a lossy

transmission line and governed by Eq. 1, 2 and 3 with  $J_D(x) = J_R = 0$ .  
Hence

$$\frac{d V(x)}{dx} = - \rho I(x) \quad (12)$$

$$\frac{d I(x)}{dx} = - g V(x) \quad (13)$$

Eq. 12 and 13 may be rewritten as

$$\frac{d^2 V(x)}{dx^2} = \rho g V(x) \quad (14)$$

$$\frac{d^2 I(x)}{dx^2} = \rho g I(x) \quad (15)$$

The solutions of Eq. 14 and 15 are

$$V(x) = A e^{\sqrt{\rho g} x} + B e^{-\sqrt{\rho g} x}$$

$$I(x) = C e^{-\sqrt{\rho g} x} + D e^{\sqrt{\rho g} x}$$

A, B, C, and D are constants of integration. The physical configuration of the cell suggests that  $I(x)$  is zero at  $x = 0$ .

Hence  $C = -D$

$$\text{and } I(x) = D [e^{\sqrt{\rho g} x} - e^{-\sqrt{\rho g} x}]$$

$$\text{or } I(x) = 2D \sinh \sqrt{\rho g} x \quad (16)$$

$$\text{Similarly } V(x) = 2D \sqrt{\rho/g} \cosh \sqrt{\rho g} x \quad (17)$$

If

$$v_e = V(x = 0)$$

$$v_a = V(x = W)$$

$$\text{and } I_a = I(x = W)$$

are known, Eq. 16 and 17 yield

$$\rho = \sqrt{V_a^2 - V_e^2} \left( \frac{1}{V I_a} \cosh^{-1} \frac{V_a}{V_e} \right) \quad (18)$$

$$g = \frac{1}{\sqrt{V_a^2 - V_e^2}} \left( \frac{I_a}{W} \cosh^{-1} \frac{V_a}{V_e} \right) \quad (19)$$

$$\text{and } V(x) = V_e \cosh \sqrt{\rho g} x \quad (20)$$

$V_a$ ,  $I_a$ ,  $V_e$  and  $W$  for a given cell can be obtained from measurements under reverse-biased condition. Hence Eq. (18) and (19) determine the unknown constants  $\rho$  and  $g$  of the model.

In order to check the validity of the model, the above values for  $\rho$  and  $g$  were substituted in Eq. 20 of the potential profile  $V(x)$  and the result plotted. The computed and measured potential profiles for a given cell in the reverse-biased case are shown in Figure 3 for three different values of  $V_a$ .

#### Determination of $J_o$ and $r$ .

The parameters  $J_o$  and  $r$  can be investigated by considering an unilluminated cell under forward-biased condition. The model for the cell for this case is shown in Figure 2c. This model is described by the following set of Equations 21, 22, and 23 which are similar to Eq. 8, 9 and 10 but with  $J_R = 0$

$$\frac{d J_D(\xi)}{d \xi} = - \frac{\rho W_a [J_D(\xi) + J_o]}{1 + r a [J_D(\xi) + J_o]} I(\xi) \quad (21)$$

$$\frac{d I(\xi)}{d \xi} = - W [g V(x) + J_D(\xi)] \quad (22)$$

$$\frac{dV}{dx} = - \rho W I(\xi) \quad (23)$$

where  $\xi = \frac{x}{W}$ .

The set of Eq. 21, 22, and 23 is a system of nonlinear, coupled, first order differential equations. There are three boundary conditions necessary for a unique solution. The boundary condition  $I_e = 0$  stems from the physical configuration and is discussed earlier. The remaining two boundary

conditions enter the problem as experimental constraints. These two boundary conditions are not independent of each other since the differential equations are coupled with each other. A knowledge of  $V_e = V(x=W)$  or  $V_a = V(x=0)$  helps to determine  $J_{De} = J_D(x=W)$  or  $J_{Da} = J_D(x=0)$  respectively from the transcendental equation (11), replacing  $V_{oc}$  by  $V_e$  or  $V_a$ .

Taking  $V_a$ ,  $J_{Da}$  and  $I_e = 0$  as the boundaries, the problem becomes a boundary value problem whereas if  $V_e$ ,  $J_{De}$  and  $I_e = 0$  are taken as boundaries, the problem becomes an initial value problem. The latter is much more suitable for numerical calculations but has the disadvantage of involving quantities which are only of minor interest, namely  $V_e$  and  $J_{De}$  in place of the directly applied quantities  $V_a$  and  $J_{Da}$ .

The system of Eq. 21, 22 and 23 is not solvable analytically. A closed form solution can be found only for  $r = g = 0$ . The equations with finite values for  $r$  and  $g$  can be solved on a digital computer with a standard program for the solution of systems of first order differential equations using Adams-Moulton's method with a Runge-Kutta starter.<sup>3</sup>

For a given cell, the measurement of a potential profile along the length of the cell,  $V(\xi)$  is made for a given forward biased voltage  $V_a$  and a current  $I_a$ . Taking  $V_e$  from these measurements, the corresponding  $J_{De}$  and  $I_e = 0$  for boundary conditions of the differential equations, knowing  $\rho$  and  $g$  and assuming some values of  $r$  and  $J_{Da}$ , the quantities  $V(\xi)$ ,  $I(\xi)$  and  $J_D(\xi)$  are obtained from the computer. The assumed values of  $r$  and  $J_{Da}$  are varied in the solution of Equations 21, 22, 23 and 11 till the computed values of  $V$  and  $I$  match with the measured values. Figure 4 shows potential profiles, computed and measured for a given cell for different values of applied forward potentials  $V$ . The resulting values of  $r$  and  $J_{Da}$  together with  $\rho$  and  $g$  computed earlier are also tabulated in the figure. Figure 5 shows  $J_D(x)$  and  $I(x)$  which correspond to the computed curve 1 of Figure 4. As  $x$  increases,  $V(x)$  increases from  $V_e$  to  $V_a$ . Since  $J_D$  depends upon  $V(x)$ ,  $J_D(x)$  increases as  $x$  increases.  $I(x)$  is zero at  $x = 0$  and increases as  $x$  increases in the negative direction.

#### OPTIMIZATION OF THE CELL GEOMETRY

It has been shown that the parameters of the model can be obtained by measuring potential profiles in a given cell under reverse-biased, forward-biased and illuminated short-circuited conditions. The model can be used for the determination of optimal cell geometries. The feasible length of a cell with one contact is limited mainly by the diffused layer resistance  $\rho$ . The length can be optimized by maximizing either the power per cell or the power density, i.e. maximum power per unit cell length. The latter approach is important for gridded cells. Before discussing these two possibilities, the loss associated with a contact will be discussed.

### Losses at the Contact

So far in the analysis, the metal contact was assumed to be of negligible width and to cause negligible loss. This assumption is valid only for large cells. In small cells the losses at the contact become an important factor. Referring to Fig. 1,  $V(x)$  under the metallic contact may be assumed to be constant and equal to  $V_a$ . It has been observed<sup>4</sup> that the metal to semiconductor contact resistance is very small and may be neglected. Since light does not reach in the part of the cell covered by the metallic contact, the light generated current in this part is zero and for normal solar cell operation this region can be lumped into a forward biased diode. Thus, the output current collected at the contact is decreased by the current flowing through the diode under the contact. Since the contact width has been added to the cell length, there will be a decrease in the current and power density of the cell.

### Optimal Length of an Ungridded Cell

The effect of the length of an ungridded cell on the performance of a solar cell can be studied by computing  $J_D(x)$  and  $I(x)$  for an illuminated cell, short-circuited between the metallic contact and the bottom of the base layer. Fig. (6) shows the variation of  $I(x)$  and  $J_D(x)$  for such a cell with  $V_{oc} = 0.53V$ . Figure (6) shows that those parts of the cell lying at a distance greater than about 1 cm do not contribute significantly to  $I(x)$ . For those parts of the cell, a significant contribution goes through  $J_D$ .

Another point of view is illustrated in Fig. (7) where the output current  $I_a$  is plotted vs the cell length for an illuminated cell for various levels of illumination. It is seen that  $I_a$  increases almost linearly up to a certain length, which depends upon the level of illumination. Then  $I_a$  levels off sharply to a constant value. For maximum short-circuit current the length of the cell is about 1 cm.

### Optimizing a Gridded Cell

For certain applications such as in limited available space, an output quantity other than the maximum power is of major interest. The power density or the output power per unit length is given by

$$P_a = \frac{P_a}{W + W_c}$$

In Fig. (8) the maximum power density is plotted against the length  $W$  of the active area of a cell for various values of  $W_c$ . As expected, the smaller the value of  $W_c$ , the larger the maximum power density.  $W_c$  is decided by laboratory techniques. The optimal cell length  $W$  follows from Fig. (8) and decides the separation between grid lines for maximum power density.

## CONCLUSIONS

The model of the solar cell developed in the paper includes five constants. These constants are computed from measurements and solutions of the differential equations describing the measurements as follows:

- (a) Measuring a set of  $V_e$ ,  $V_a$  and  $I_a$  of the reverse-biased cell. Computing  $\rho$  and  $g_e$  from these measurements.
- (b) Measuring  $V_e$ ,  $V_a$  and  $I_a$  of the forward-biased cell. Computing  $r$  and  $J_o$  from the measurements and differential equations.
- (c) Measuring  $V_{oc}$  of the illuminated cell. Computing  $J_R$ .

The following conclusions may be drawn:

- (a) The computed potential profiles of the cell are in agreement with measurements.
- (b) Output current and power can be computed as a function of the length of the active area of the illuminated cell.
- (c) The output power density can be computed as a function of the area of the active length and width of contact strip.

The above analysis can be used to optimize the grid structure in a cell by making the three sets of measurements and programming the solutions on a digital computer.

REFERENCES

1. Wolf, M., "Limitations and Possibilities for Improvement of Photo-voltaic Solar Energy Converters", Proc. IRE, page 1246, (July, 1960).
2. Lamorte, M. F., "Internal Power Dissipation in Gallium Arsenide Solar Cells", Adv. En. Conv. 3, 551-563 (1963).
3. Henrici Peters, Discrete Variable Methods in Ordinary Differential Equations, Willey and Sons (1962).
4. Ralph, E. L., and P. Berman, "Silicon Cells for use in Concentrated Solar Energy", 17th Annual Power Sources Conf., pages 1-4 (1962).

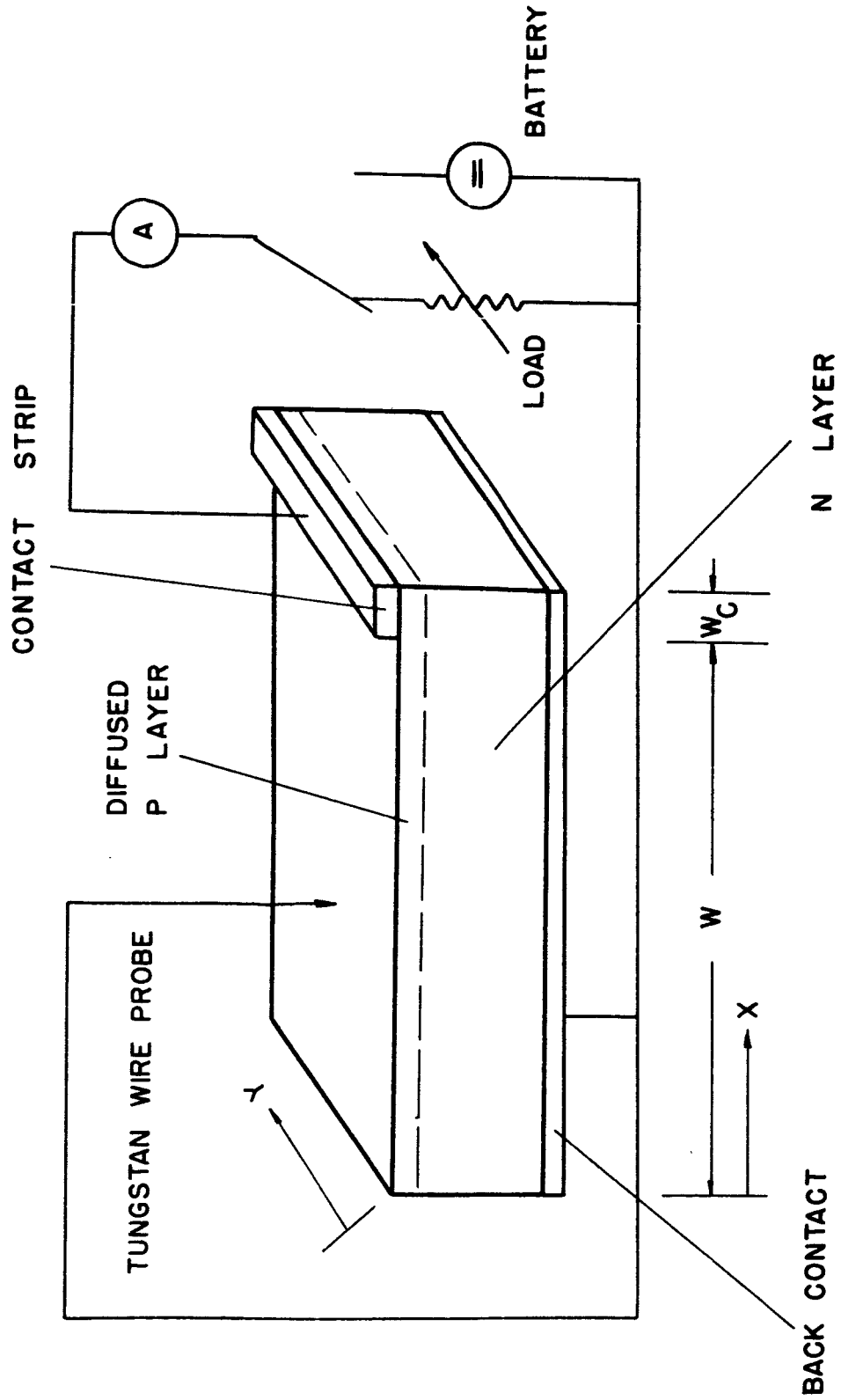
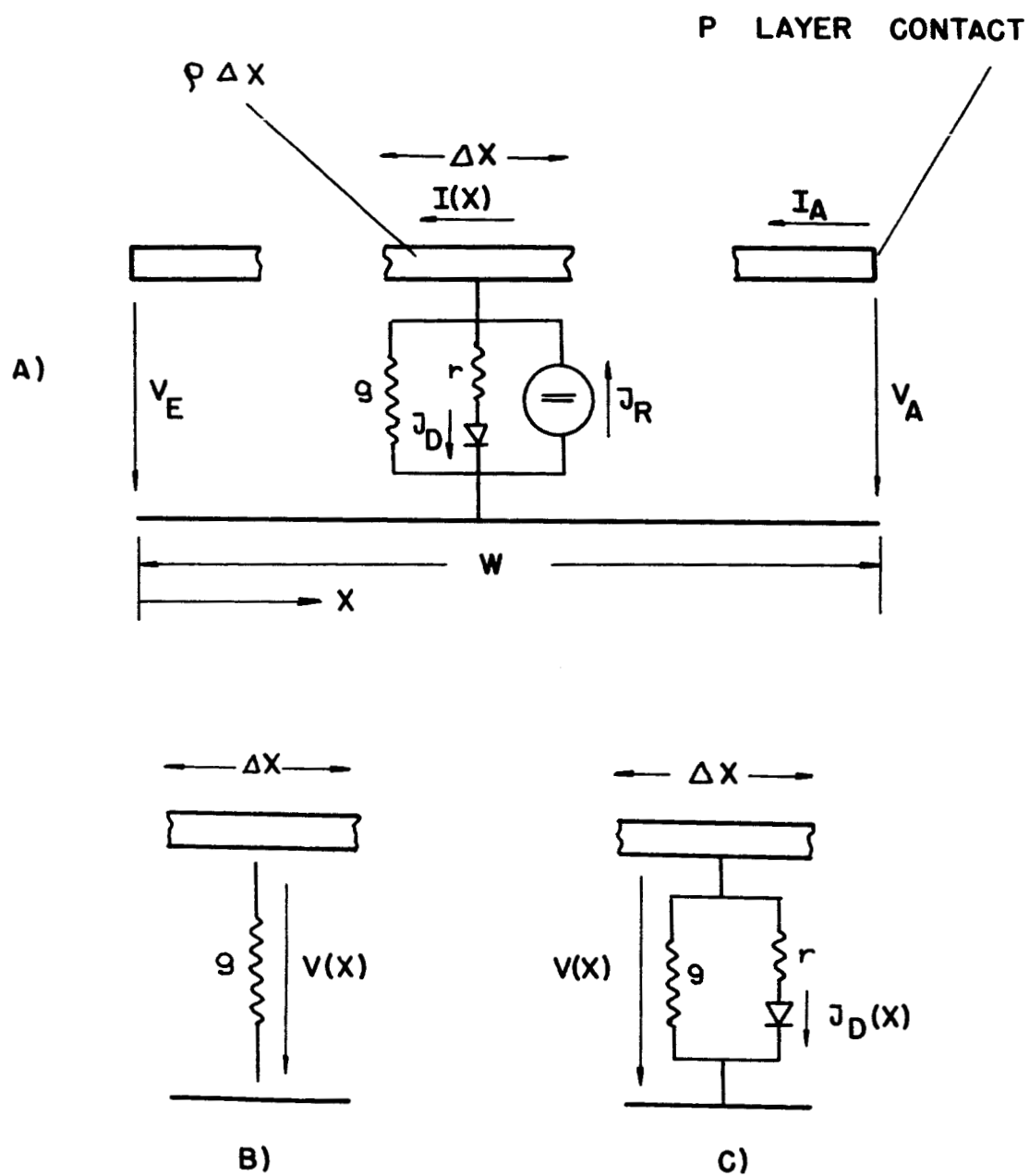


FIGURE 1. Solar Cell and Experiments

FIGURE 2. Model Configurations



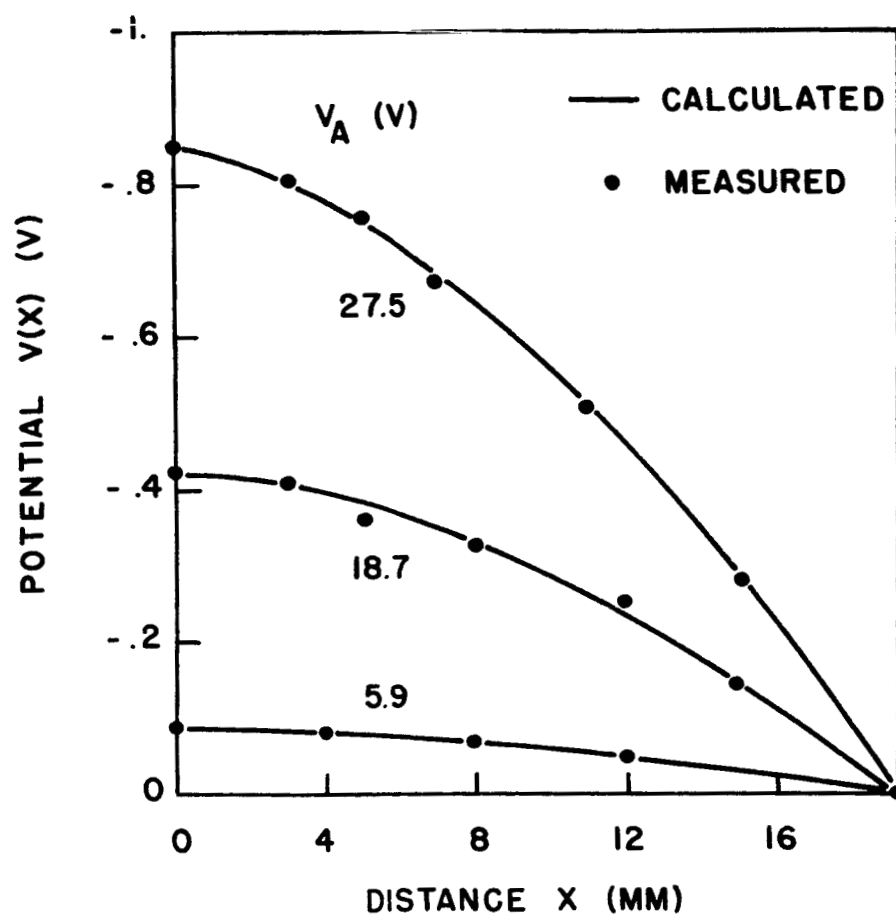


FIGURE 3. Potential Profiles Under Dark,  
Reverse Biased Condition

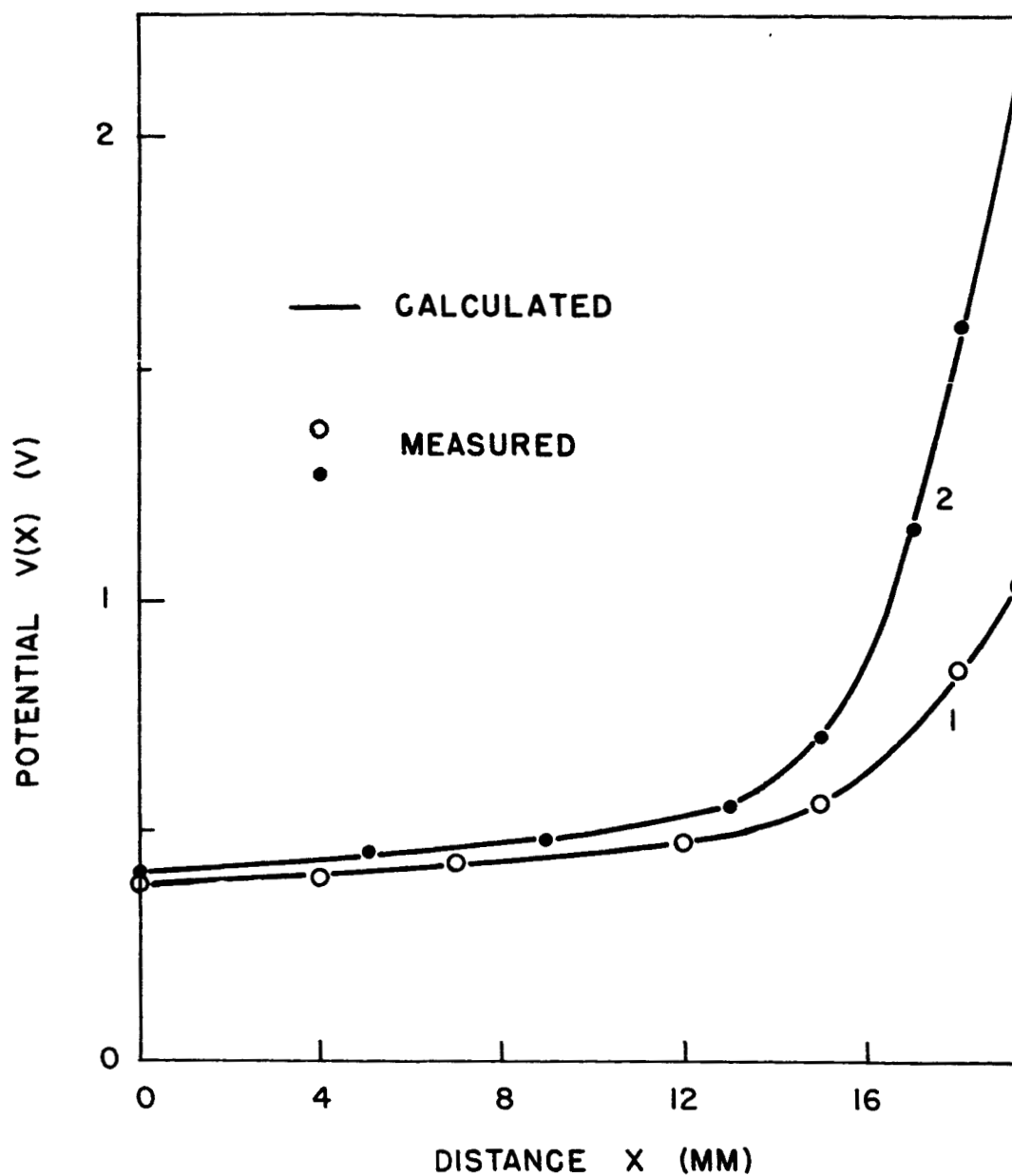


FIGURE 4. Forward Potential Profiles Under Dark Condition  
for the Final Model

No.	$g$	$\rho$	$r$	$J_0$
1	$0.623 \cdot 10^{-5}$	16	84	$0.49 \cdot 10^{-11}$
2	"	"	"	"
	( $1/\Omega \text{ mm}$ )	( $\Omega/\text{mm}$ )	( $\Omega/\text{mm}$ )	(A/mm)

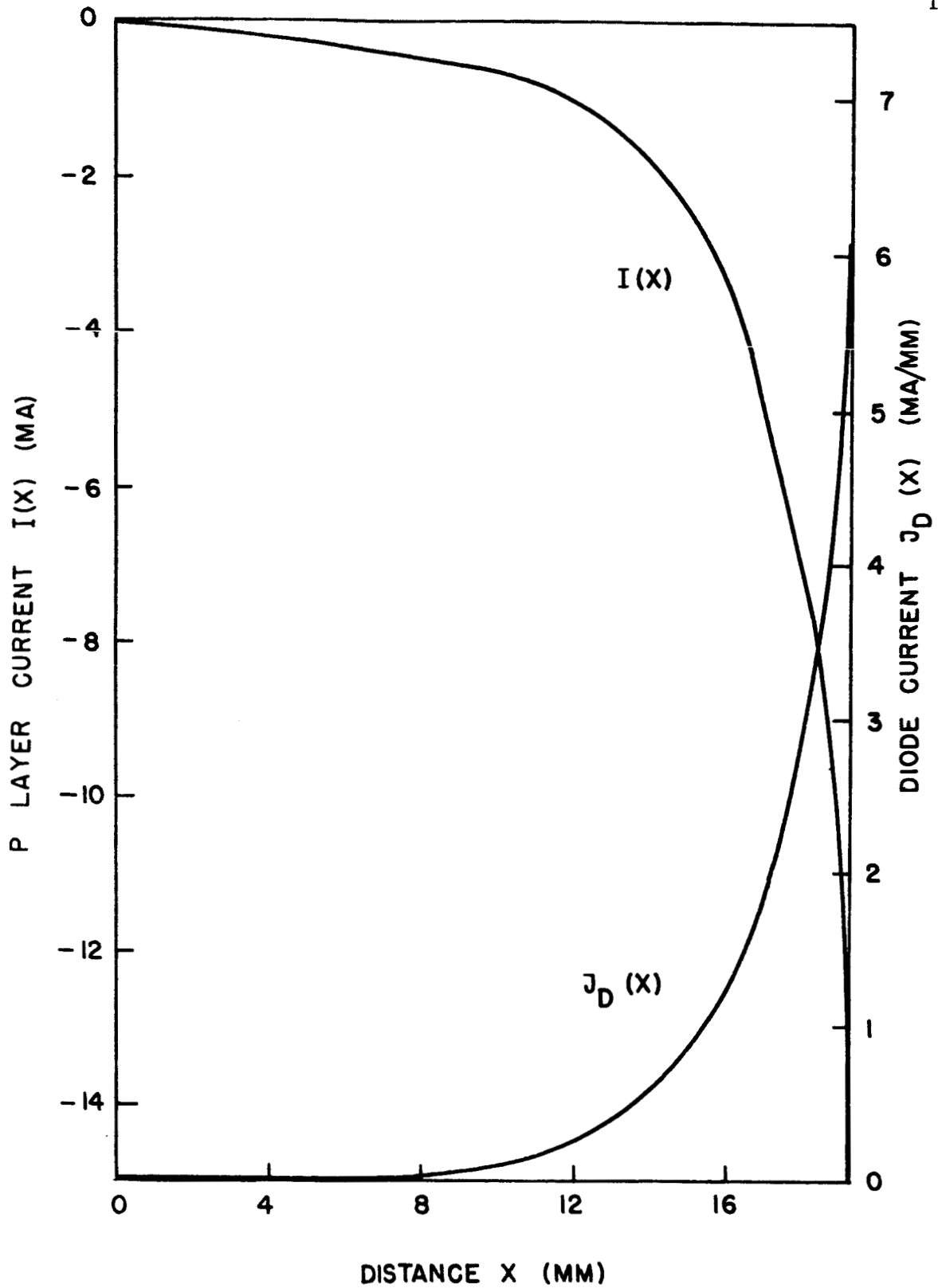


FIGURE 5. Calculated Diode- and P-Layer-Current Under Dark, Forward Biased Condition (Corresponding to Curve 1 in Figure 4)

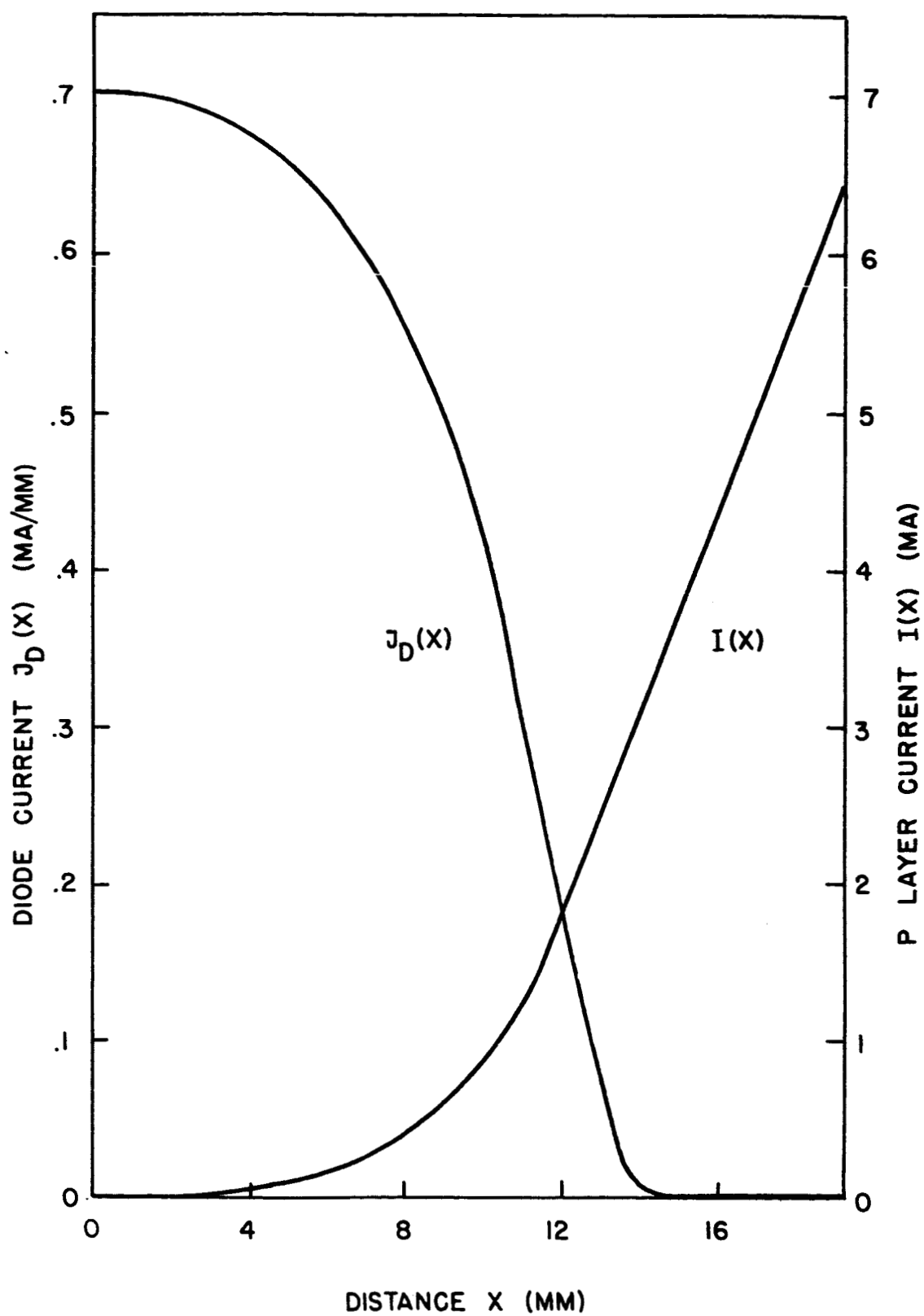


FIGURE 6. Calculated Diode- and P-Layer-Currents. Illuminated, Short-Circuit Condition.  $V_{oc} = 0.53$  V.

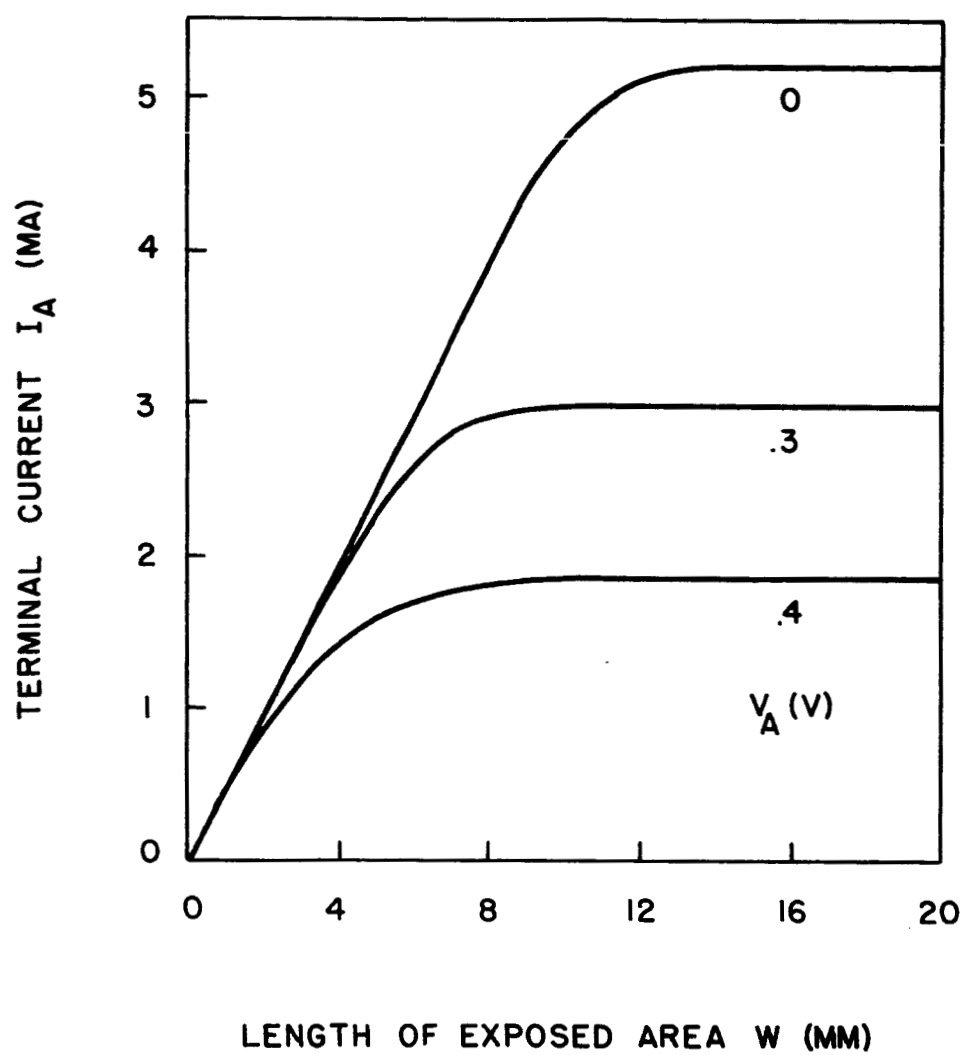


FIGURE 7. Output Currents for the  
Illuminated Cell.  $V_{oc} = 0.5$  V.

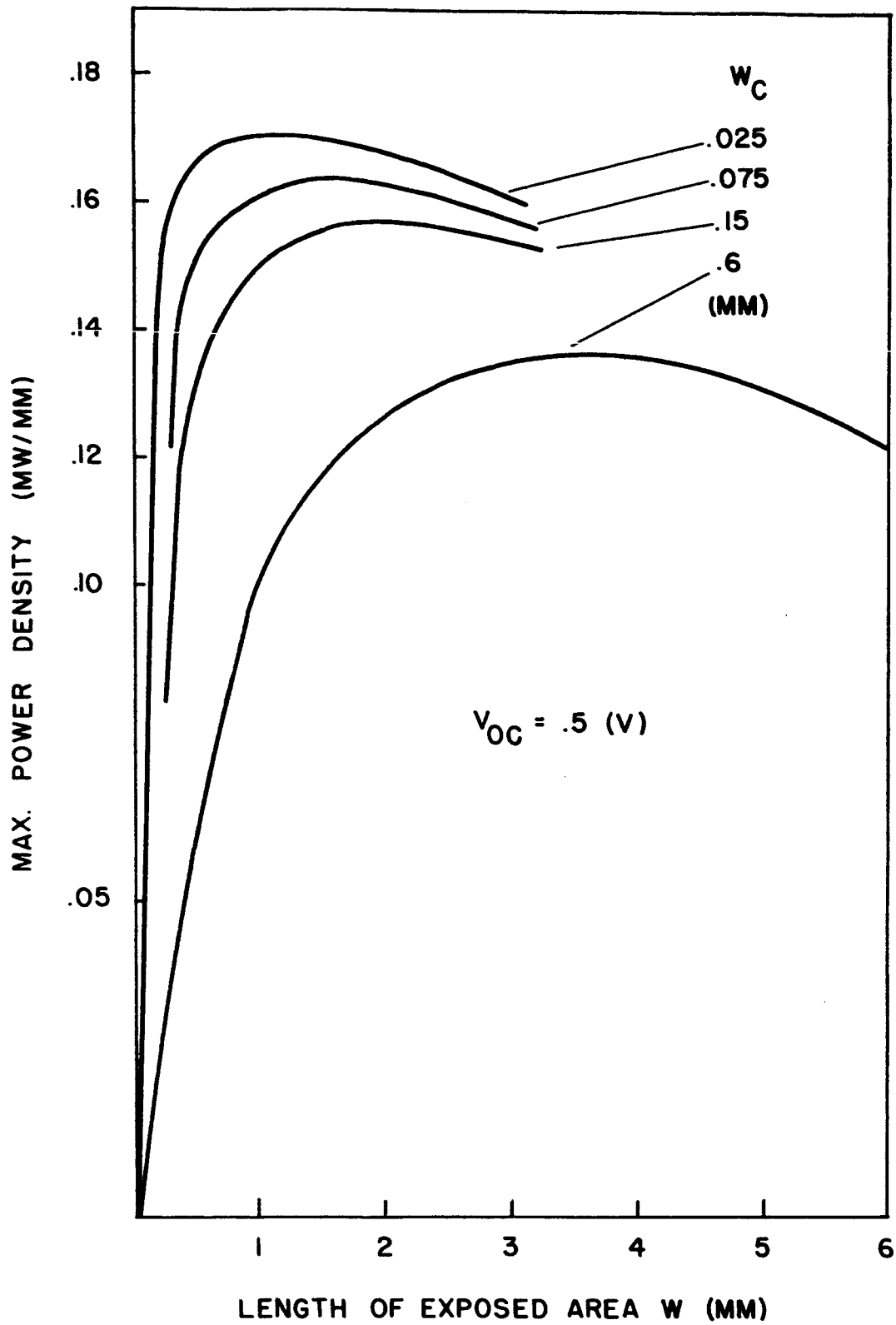


FIGURE 8. Maximum Power Density for the Illuminated Cell.